DOI 10.1007/s10778-016-0757-3
International Applied Mechanics, Vol. 52, No. 4, July, 2016

ANALYSIS OF THE STRESS–STRAIN STATE OF INHOMOGENEOUS HOLLOW CYLINDERS

A. Ya. Grigorenko and S. N. Yaremchenko

The stress–strain state of an inhomogeneous hollow cylinder with different boundary conditions at the ends is analyzed using the three-dimensional theory of elasticity. Spline collocation is used to reduce the two-dimensional boundary-value problem to a boundary-value problem for a system of ordinary differential equations of high order with respect to the radial coordinate, which is solved with the stable discrete-orthogonalization method. The results obtained using the spline-collocation, Fourier-series, and finite-element methods are compared

Keywords: stress–strain state, three-dimensional theory of elasticity, hollow cylinder, finite length, spline-collocation, finite-element method

Introduction. The strict requirements to strength analysis, the tendency to detailing the real properties of structural materials, and the consideration of three-dimensional effects in thick-walled structural members necessitate studying hollow cylindrical structures in three dimensions. The stress–strain analysis of thick-walled structures based on the three-dimensional theory of elasticity involves severe difficulties associated with the complexity of the starting systems of partial differential equations and the necessity to satisfy boundary conditions on the surface of an elastic body.

These difficulties are even more severe when designing cylindrical elements made of anisotropic and inhomogeneous materials, such as functionally graded materials (FGM) with variable elastic characteristics.

Modern technologies make it possible to produce structures with required smoothly varying elastic moduli. The physical and mechanical properties of FGMs based on various compositions are addressed in [3, 11–13]. Of great practical interest and importance for fundamental research is the analysis of the stress–strain state of various structural members made of FGMs, including finite-length cylinders. In view of the above, it is necessary to determine the dynamic characteristics of such structural members in three dimensions. Due to great computational difficulties, there are only few publications on the three-dimensional stress–strain state of elastic bodies made of FGMs [4, 10, 14].

Along with such universal methods as finite-difference, finite-element, and other discrete methods used to solve boundary-value problems of mechanics and mathematical physics, there are methods that reduce the original problem to a system of ordinary differential equations using analytical approximation of the solution. Reducing multidimensional problems to one-dimensional ones and using the stable numerical discrete-orthogonalization method, we obtain the required results with high accuracy [6, 9].

The spline-approximation method was used in [5, 6, 8] to analyze the stress–strain state of shells and thick plates. The main advantages of splines are stability against local perturbations (i.e., the local behavior of a spline near a point does not influence its overall behavior, in contrast to, for example, polynomial approximation), good convergence, and simple and convenient computer implementation.

Here we will analyze the axisymmetric stress state of hollow cylinders that can be described by a two-dimensional boundary-value problem [7]. We will assume that the elastic modulus can vary in the radial direction. Therefore, spline

S. P. Timoshenko Institute of Mechanics, National Academy of Sciences of Ukraine, 3 Nesterova St., Kyiv, Ukraine 03057, e-mail: ayagrigorenko@yandex.ru. Translated from Prikladnaya Mekhanika, Vol. 52, No. 4, pp. 16–24, July–August, 2016. Original article submitted June 5, 2015.

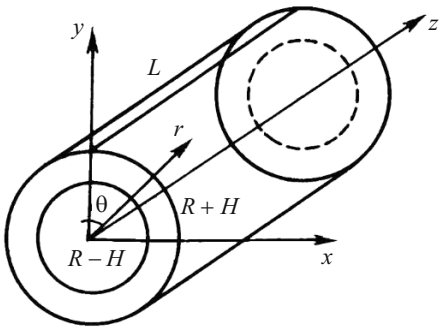

Fig. 1

approximation will be performed along the length of the cylinder. Doing so leads to a one-dimensional boundary-value problem in the radial direction. We will compare the results obtained by the above method with those obtained by the finite-element method and (for some problems) the Fourier-series method.

1. Problem Formulation. Basic Equations. Consider a hollow orthotropic cylinder with inner radius $R-H$, outer radius $R+H$ (R is the midsurface radius, $2H$ is the cylinder thickness), and length L described in cylindrical coordinates r, θ, z (Fig. 1). The axisymmetric stress–strain state of the cylinder is described by the kinematic equations

$$e_r = \frac{\partial u_r}{\partial r}, \quad e_\theta = \frac{u_r}{r}, \quad e_z = \frac{\partial u_z}{\partial z}, \quad 2e_{rz} = \frac{\partial u_r}{\partial z} + \frac{\partial u_z}{\partial r}, \tag{1}$$

Hooke's law

$$\sigma_r = \lambda_{11} e_r + \lambda_{12} e_\theta + \lambda_{13} e_z, \quad \sigma_\theta = \lambda_{12} e_r + \lambda_{22} e_\theta + \lambda_{23} e_z,$$
$$\sigma_z = \lambda_{13} e_r + \lambda_{23} e_\theta + \lambda_{33} e_z, \quad \sigma_{rz} = 2\lambda_{55} e_{rz}, \tag{2}$$

where $\lambda_{ij} = \lambda_{ij}(r, z)$ are the elements of the stiffness matrix, which are differentiable continuous functions of the coordinates r and z,

and the equilibrium equations

$$\frac{\partial \sigma_r}{\partial r} + \frac{\partial \sigma_{rz}}{\partial z} + \frac{\sigma_r - \sigma_\theta}{r} = 0,$$
$$\frac{\partial \sigma_{rz}}{\partial r} + \frac{\partial \sigma_z}{\partial z} + \frac{\sigma_{rz}}{r} = 0, \tag{3}$$

where $u_r(r, z)$ and $u_z(r, z)$ are the projections of the displacement vector onto the r- and z-axes; e_r, e_θ, and e_z are the relative linear strains along the coordinate lines; e_{rz} are the shear strains; $\sigma_r, \sigma_\theta, \sigma_z$ are the normal stresses; σ_{rz} are the tangential stresses.

If the body is isotropic, the elements of the stiffness matrix become

$$\lambda_{11} = \lambda_{22} = \lambda_{33} = \lambda + 2\mu, \quad \lambda_{12} = \lambda_{13} = \lambda_{23} = \lambda, \quad \lambda_{55} = \mu, \tag{4}$$

where $\mu = \dfrac{E}{2(1+\nu)}$, $\lambda = \dfrac{2\mu\nu}{(1-2\nu)}$; ν and E are Poisson's ratio and Young's modulus.

The boundary conditions on the inside ($r = R-H$) and outside ($r = R+H$) surfaces of the cylinder are

$$\sigma_r(R-H, z) = q_1, \quad \sigma_r(R+H, z) = q_2, \quad \sigma_{rz}(R \pm H, z) = 0. \tag{5}$$

The following boundary conditions can be specified at the cylinder ends $z = 0$ and $z = L$:

(i) $$\sigma_z = 0, \quad u_r = 0 \quad \text{or} \quad \frac{\partial u_z}{\partial z} = 0, \quad u_r = 0 \,(\text{hinging}) \tag{6}$$

(ii) $$u_z = 0, \quad \frac{\partial u_r}{\partial z} = 0 \,(\text{symmetry}) \tag{7}$$

(iii) $$u_r = 0, \quad u_z = 0 \,(\text{clamping}). \tag{8}$$

The governing equations for displacements take the form

$$\frac{\partial^2 u_r}{\partial r^2} = \left(-\frac{1}{\lambda_{11}} \frac{\partial \lambda_{12}}{\partial r} \frac{1}{r} + \frac{\lambda_{22}}{\lambda_{11}} \frac{1}{r^2} \right) u_r - \frac{1}{\lambda_{11}} \frac{\partial \lambda_{55}}{\partial z} \frac{\partial u_r}{\partial z} - \frac{\lambda_{55}}{\lambda_{11}} \frac{\partial^2 u_r}{\partial z^2}$$

$$- \left(\frac{1}{\lambda_{11}} \frac{\partial \lambda_{11}}{\partial r} + \frac{1}{r} \right) \frac{\partial u_r}{\partial r} - \left(\frac{1}{\lambda_{11}} \frac{\partial \lambda_{13}}{\partial r} - \frac{\lambda_{23} - \lambda_{32}}{\lambda_{11}} \frac{1}{r} \right) \frac{\partial u_z}{\partial z} - \frac{1}{\lambda_{11}} \frac{\partial \lambda_{55}}{\partial z} \frac{\partial u_z}{\partial r} - \frac{\lambda_{13} + \lambda_{55}}{\lambda_{11}} \frac{\partial^2 u_z}{\partial z \partial r},$$

$$\frac{\partial^2 u_z}{\partial r^2} = -\frac{1}{\lambda_{55}} \frac{\partial \lambda_{23}}{\partial z} \frac{u_r}{r} - \left(\frac{1}{\lambda_{55}} \frac{\partial \lambda_{55}}{\partial r} + \frac{\lambda_{23}}{\lambda_{55}} \frac{1}{r} + \frac{1}{r} \right) \frac{\partial u_r}{\partial z}$$

$$- \left(1 + \frac{\lambda_{13}}{\lambda_{55}} \right) \frac{\partial^2 u_r}{\partial r \partial z} - \frac{1}{\lambda_{55}} \frac{\partial \lambda_{13}}{\partial z} \frac{\partial u_r}{\partial r} - \frac{1}{\lambda_{55}} \frac{\partial \lambda_{33}}{\partial z} \frac{\partial u_z}{\partial z} - \frac{\lambda_{33}}{\lambda_{55}} \frac{\partial^2 u_z}{\partial z^2} - \left(\frac{1}{r} + \frac{1}{\lambda_{55}} \frac{\partial \lambda_{55}}{\partial r} \right) \frac{\partial u_z}{\partial r}. \tag{9}$$

Transforming Eq. (9), we get

$$\frac{\partial^2 u_r}{\partial r^2} = a_{11} u_r + a_{12} \frac{\partial u_r}{\partial z} + a_{13} \frac{\partial^2 u_r}{\partial z^2} + a_{14} \frac{\partial u_r}{\partial r} + a_{15} \frac{\partial u_z}{\partial z} + a_{16} \frac{\partial u_z}{\partial r} + a_{17} \frac{\partial^2 u_z}{\partial r \partial z},$$

$$\frac{\partial^2 u_z}{\partial r^2} = a_{21} u_r + a_{22} \frac{\partial u_r}{\partial z} + a_{23} \frac{\partial u_r}{\partial r} + a_{24} \frac{\partial^2 u_r}{\partial r \partial z} + a_{25} \frac{\partial u_z}{\partial z} + a_{26} \frac{\partial^2 u_z}{\partial z^2} + a_{27} \frac{\partial u_z}{\partial r}, \tag{10}$$

where the coefficients $a_{kl} = a_{kl}(r, z)$ are expressed as

$$a_{11} = -\frac{1}{\lambda_{11} r} \frac{\partial \lambda_{12}}{\partial r} + \frac{\lambda_{22}}{\lambda_{11} r^2}, \quad a_{12} = -\frac{1}{\lambda_{11}} \frac{\partial \lambda_{55}}{\partial z}, \quad a_{13} = -\frac{\lambda_{55}}{\lambda_{11}}, \quad a_{14} = -\left(\frac{1}{\lambda_{11}} \frac{\partial \lambda_{11}}{\partial r} + \frac{1}{r} \right),$$

$$a_{15} = -\left(\frac{1}{\lambda_{11}} \frac{\partial \lambda_{13}}{\partial r} - \frac{\lambda_{23} - \lambda_{13}}{\lambda_{11} r} \right), \quad a_{16} = -\frac{1}{\lambda_{11}} \frac{\partial \lambda_{55}}{\partial z}, \quad a_{17} = -\frac{\lambda_{13} - \lambda_{55}}{\lambda_{11}},$$

$$a_{21} = -\frac{1}{\lambda_{55} r} \frac{\partial \lambda_{23}}{\partial z}, \quad a_{22} = -\left(\frac{1}{\lambda_{55}} \frac{\partial \lambda_{55}}{\partial r} + \frac{\lambda_{23}}{\lambda_{55}} \frac{1}{r} + \frac{1}{r} \right), \quad a_{23} = -\frac{1}{\lambda_{55}} \frac{\partial \lambda_{13}}{\partial z},$$

$$a_{24} = -\left(1 + \frac{\lambda_{13}}{\lambda_{55}} \right), \quad a_{25} = -\frac{1}{\lambda_{55}} \frac{\partial \lambda_{33}}{\partial z}, \quad a_{26} = -\frac{\lambda_{33}}{\lambda_{55}}, \quad a_{27} = -\left(\frac{1}{r} + \frac{1}{\lambda_{55}} \frac{\partial \lambda_{55}}{\partial r} \right). \tag{11}$$

The boundary conditions are

$$\lambda_{11} \frac{\partial u_r}{\partial r} + \lambda_{12} \frac{u_r}{r} + \lambda_{13} \frac{\partial u_z}{\partial z} = q_1, \quad \lambda_{55} \left(\frac{\partial u_r}{\partial z} + \frac{\partial u_z}{\partial r} \right) = 0, \tag{12}$$

$$\lambda_{11} \frac{\partial u_r}{\partial r} + \lambda_{12} \frac{u_r}{r} + \lambda_{13} \frac{\partial u_z}{\partial z} = q_2, \quad \lambda_{55} \left(\frac{\partial u_r}{\partial z} + \frac{\partial u_z}{\partial r} \right) = 0. \tag{13}$$

2. Procedure for Solution of Boundary-Value Problems. The boundary-value problem (10) with the appropriate boundary conditions can be solved by the spline-collocation method. To this end, we represent the unknown functions $u_r(r,z)$ and $u_z(r,z)$ as

$$u_r = \sum_{i=0}^{N} u_{ri}(r)\varphi_i^{(1)}(z), \qquad u_z = \sum_{i=0}^{N} u_{zi}(r)\varphi_i^{(2)}(z), \tag{14}$$

where $u_{ri}(r)$ and $u_{zi}(r)$ are unknown functions of r; $\varphi_i^{(j)}(z)$ $(j=1,2,\ i=0,1,\dots,N)$ are linear combinations of normalized B-splines over a uniform mesh Δ: $z_{-3} < z_{-2} < z_{-1} < 0 = z_0 < z_1 < \dots < z_N = L < z_{N+1} < z_{N+2} < z_{N+3}$, subject to the boundary conditions at $z=0$ and $z=L$.

System (11) includes no higher than 2nd-order derivatives of the unknown functions with respect to z; therefore, it is sufficient to use cubic splines.

Substituting (14) into Eqs. (10), we require them to hold at the given collocation points $\xi_k \in [0,L]$, $k=0,N$. Let the mesh have an even number of nodes, i.e., $N=2n+1$ $(n\ge 3)$. We select the collocation points so that $\xi_{2i} \in [z_{2i}, z_{2i+1}]$, $\xi_{2i+1} \in [z_{2i}, z_{2i+1}]$ $(i=0,1,2,\dots,n)$, with $\xi_{2i} = z_{2i} + s_1 h_z$, $\xi_{2i+1} = z_{2i} + s_2 h_z$, where $s_1 = 1/2 - \sqrt{3}/6$ and $s_2 = 1/2 + \sqrt{3}/6$ are the roots of a Legendre polynomial of the second order. This choice is optimal and improves the accuracy of the approximation. In this case, the number of collocation points is $N+1$. Finally, we obtain a system of $4(N+1)$ linear differential equations for the functions $u_{ri}, \tilde{u}_{ri}, u_{zi}, \tilde{u}_{zi}$ $(i=0,\dots,N)$, where $\tilde{u}_{ri} = u'_{ri}$ and $\tilde{u}_{zi} = u'_{zi}$.

Denote

$$\Phi_j = [\varphi_i^{(j)}(\xi_k)], \qquad k,i=0,\dots,N, \qquad j=1,2,$$

$$\bar{u}_r = \{u_{r0}, u_{r1}, \dots, u_{rN}\}^T, \qquad \bar{\tilde{u}}_r = \{\tilde{u}_{r0}, \tilde{u}_{r1}, \dots, \tilde{u}_{rN}\}^T,$$

$$\bar{u}_z = \{u_{z0}, u_{z1}, \dots, u_{zN}\}^T, \qquad \bar{\tilde{u}}_z = \{\tilde{u}_{z0}, \tilde{u}_{z1}, \dots, \tilde{u}_{zN}\}^T,$$

$$\bar{a}_{kl}^T = \{a_{kl}(r,\xi_0), a_{kl}(r,\xi_1), \dots, a_{kl}(r,\xi_N)\}. \tag{15}$$

The matrix $[c_i a_{ij}]$ is denoted by $\bar{c} * A$, where $A = [a_{ij}]$ $\{i,j=0,\dots,N\}$, and $\bar{c} = \{c_0, c_1, \dots, c_N\}^T$. Then the system of ordinary differential equations for $u_{ri}, \tilde{u}_{ri}, u_{zi}, \tilde{u}_{zi}$ becomes

$$\frac{d\bar{u}_r}{dr} = \bar{\tilde{u}}_r, \qquad \frac{d\bar{u}_z}{dr} = \bar{\tilde{u}}_z,$$

$$\frac{d\bar{\tilde{u}}_r}{dr} = \Phi_1^{-1}(\bar{a}_{11} * \Phi_1 + \bar{a}_{12} * \Phi_1' + \bar{a}_{13} * \Phi_1'')\bar{u}_r + \Phi_1^{-1}(\bar{a}_{14} * \Phi_1)\bar{\tilde{u}}_r$$

$$+ \Phi_1^{-1}(\bar{a}_{15} * \Phi_2')\bar{u}_z + \Phi_1^{-1}(\bar{a}_{16} * \Phi_2 + \bar{a}_{17} * \Phi_2')\bar{\tilde{u}}_z,$$

$$\frac{d\bar{\tilde{u}}_z}{dy} = \Phi_2^{-1}(\bar{a}_{21}\Phi_1 + \bar{a}_{22}\Phi_1')\bar{u}_r + \Phi_2^{-1}(\bar{a}_{23} * \Phi_1')\bar{\tilde{u}}_r$$

$$+ \Phi_2^{-1}(\bar{a}_{24} * \Phi_2 + \bar{a}_{25} * \Phi_2' + \bar{a}_{26} * \Phi_2'')\bar{u}_z + \Phi_2^{-1}(\bar{a}_{27} * \Phi_2)\bar{\tilde{u}}_z \tag{16}$$

or in brief form:

$$\frac{d\bar{Y}}{dr} = A(r)\bar{Y} \qquad (R-H \le r \le R+H), \tag{17}$$

where $\bar{Y} = \{u_{r_0}, \dots u_{rN}, \tilde{u}_{r0}, \dots, \tilde{u}_{rN}, u_{z0}, \dots, u_{zN}, \tilde{u}_{zo}, \dots, \tilde{u}_{zN}\}^T$ is a vector function of r; $A(r)$ is a $4(N+1)\times 4(N+1)$ -matrix.

The boundary conditions for this system are given by

$$B_1\bar{Y}(R-H)=\bar{b}_1, \qquad B_2\bar{Y}(R+H)=\bar{b}_2, \tag{18}$$

where B_1 and B_2 are $2(N+1)\times 4(N+1)$-matrices; $\bar{b}_1$ and $\bar{b}_2$ are the respective vectors.

The boundary-value problem (17), (18) is solved by the discrete-orthogonalization method. With the boundary conditions (6), the problem can be solved by expanding the unknown functions into Fourier series:

$$u_r = \sum_{m=1,\,3,\,5,\ldots}^{M} u_{rm}(r)\sin\frac{m\pi z}{L}, \qquad u_z = \sum_{m=1,\,3,\,5,\ldots}^{M} u_{zi}(r)\cos\frac{m\pi z}{L}. \tag{19}$$

Substituting expressions (19) into Eqs. (10) and the boundary conditions (12), (13), we obtain a sequence of one-dimensional boundary-value problems for the unknown functions $u_{rm}(r)$ and $u_{zm}(r)$, which are solved by the discrete-orthogonalization method.

In the case of clamped boundary conditions, the finite-element method (FEM) can be used [1]. If pressure (5) acts on the inside and outside surfaces of the cylinder, the strain energy is expressed as

$$\Pi = 2\pi\int_0^L\int_{R-H}^{R+H}\left\{\frac{1}{2}\left(\sigma_r e_r+\sigma_z e_z+\sigma_\theta e_\theta\right)+\sigma_{rz}e_{rz}\right\}rdzdr$$

$$+2\pi(R-H)\int_0^L q_1 u_r dz-2\pi(R+H)\int_0^L q_2 u_r dz. \tag{20}$$

Using the boundary conditions (6)–(8) for displacements and expressing stresses and strains in terms of the displacements from (1), (2), and (4), we get

$$\Pi=\int_0^L\int_{R-H}^{R+H}\frac{\pi}{r}\left\{r^2(\lambda+2\mu)\left(\frac{\partial u_r}{\partial r}\right)^2+2r\lambda u_r\frac{\partial u_r}{\partial r}+2r^2\lambda\frac{\partial u_z}{\partial z}\frac{\partial u_r}{\partial r}\right.$$

$$+2r\lambda u_r\frac{\partial u_z}{\partial z}+r^2(\lambda+2\mu)\left(\frac{\partial u_z}{\partial z}\right)^2+(\lambda+2\mu)u_r^2+\mu r^2\left(\frac{\partial u_r}{\partial z}\right)^2$$

$$\left.+2\mu r^2\frac{\partial u_r}{\partial z}\frac{\partial u_z}{\partial r}+\mu r^2\left(\frac{\partial u_z}{\partial r}\right)^2\right\}dzdr+2\pi(R-H)\int_0^L q_1u_r dz-2\pi(R+H)\int_0^L q_2u_r dz. \tag{21}$$

We will use four-node finite elements [1]. The use of second-order polynomials, i.e., eight-node finite elements, to approximate the solution of a thermoviscoelastic problem was detailed in [2]. Calculations show that four terms in the series are sufficient to solve the problem. The integration is carried out using three-point Gaussian quadratures for one-dimensional integrals and nine-point quadratures for double integrals. The resulting systems of linear algebraic equations can be solved by Gaussian elimination.

3. Analysis of the Numerical Results. Let us use the above approach to determine the stress–strain state of hollow cylinders with the following parameters: length $L=5$, inner radius $R-H=3$, outer radius $R+H=5$, Poisson's ratio $\nu=0.4$, elastic modulus $E(r)=ar^2+br+c$. Consider the following cases:

(i) increasing Young's modulus ($E(R-H)=11E_0/15$, $E(R)=E_0$, $E(R+H)=81E_0/50$, $a=0.1767$, $b=-0.97$, $c=2.053$);

(ii) decreasing Young's modulus ($E(R-H)=81E_0/50$, $E(R)=E_0$, $E(R+H)=11E_0/15$, $a=0.1767$, $b=-1.857$, $c=5.6$);

(iii) thickness-average Young's modulus ($E=1.0589E_0$).

TABLE 1

r	Spline -collocation			FEM	Fourier series
	$N = 39$	$N = 49$	$N = 59$		
3	3.188	3.172	3.161	3.044	3.081
4	0.6129	0.6095	0.6073	0.5958	0.5966
5	–1.337	–1.336	–1.335	–1.329	–1.331

TABLE 2

r	Spline -collocation			FEM	Fourier series
	$N = 39$	$N = 49$	$N = 59$		
3	5.612	5.606	5.602	5.578	5.58
4	4.89	4.882	4.877	4.85	4.853
5	4.054	4.047	4.042	4.017	4.02

Let normal uniform pressure q act on the inside surface of the shell. Then $q_1 = -q$ and $q_2 = 0$ in the boundary conditions (5). Let us compare the results obtained for the boundary conditions (6) and Young's modulus (i) using the Fourier-series, finite-element, and spline-collocation methods. Let $M = 55$ in the Fourier series (19). The interval of integration is partitioned into 200 subintervals (doubling them does not improve the result). Since the problem is symmetric, it can be solved on the interval $[0, L/2]$ when using the spline-collocation and finite-element methods. Therefore, for the spline-collocation method, conditions (6) are used at $z = 0$ and conditions (7) at $z = L/2$, and the interval of integration is partitioned into 400 subintervals. For the FEM, the domain is partitioned into 0.1×0.1 finite elements with $u_r = 0$ at the nodal points for which $z = 0$ and $u_z = 0$ at the nodal points for which $z = L/2$. Tables 1 and 2 collect the values of the displacements $\hat{u}_z = u_z E_0 / q$ for $z = 0$ and $\hat{u}_r = u_r E_0 / q$ for $z = L/2$ for different problem-solving methods and the following values of the parameter N in (14): 39, 49, 59 (i.e., 40, 50, 60 collocation points, respectively).

It can be seen that the results obtained by the different methods differ insignificantly. The greater the number of collocation points, the less the difference.

The solution of the problem for the same shell with clamped ends under the same loading. Figures 2 and 3 show the distribution of the displacement $\hat{u}_z$ in the section $z = 1$ and the distribution of the displacement $\hat{u}_r$ in the section $z = L/2$, respectively. The numbers near the curves correspond to the cases of elastic moduli, the solid lines to the spline-collocation method, and the triangles to the FEM (the size of finite elements is the same as in the case of hinged support).

As can be seen, the curves for cases (i) and (ii) differ insignificantly, while the curve for case (iii) is between them. The values of $\hat{u}_z$ obtained with the finite-element and spline-collocation methods are in good agreement, whereas the difference between the values of $\hat{u}_r$ is greater.

Let now pressure be applied to the outside surface of the cylinder and its ends be clamped. Then $q_2 = -q$ and $q_1 = 0$ in the boundary conditions (5).

Figures 4 and 5 show the distribution of the displacement $\hat{u}_z$ in the section $z = 1$ and the distribution of the displacement $\hat{u}_r$ in the section $z = L/2$, respectively. The notation here is the same as in the previous example. As in the previous case, the displacement $\hat{u}_z$ is weakly dependent on the elastic modulus, while the dependence of $\hat{u}_r$ on the elastic modulus is stronger.

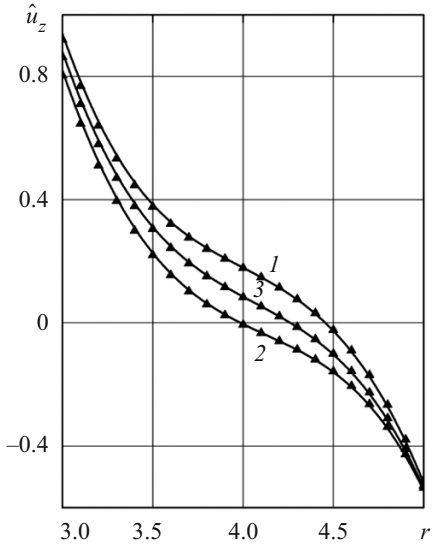

Fig. 2

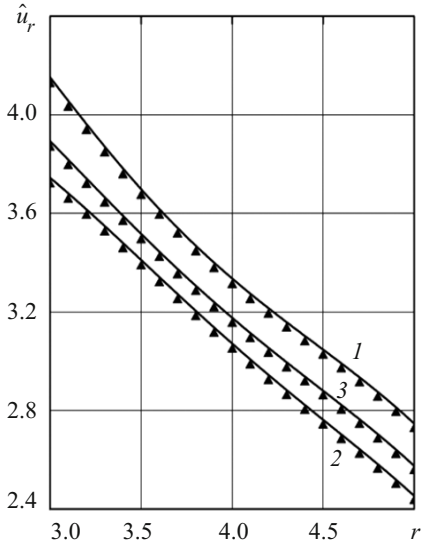

Fig. 3

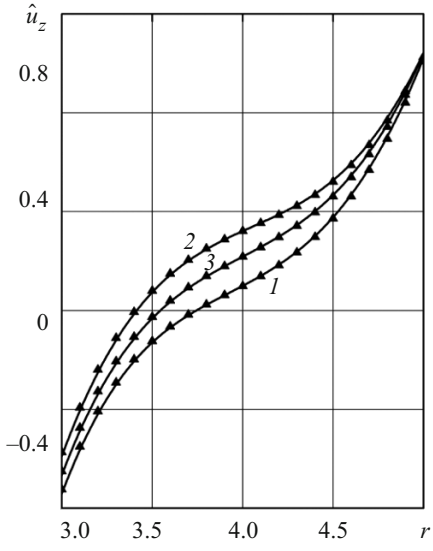

Fig. 4

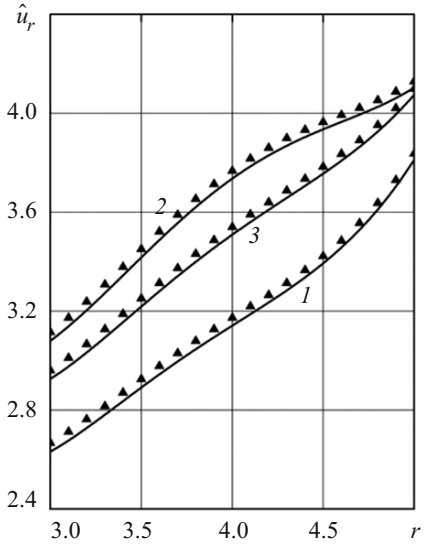

Fig. 5

The difference between the results obtained with the finite-element method (with 0.1×0.1 finite elements) and the spline-collocation method is greater in this case. The results obtained using 0.05×0.05 finite elements are shown by triangles.

Conclusions. The problems of the axisymmetric deformation of inhomogeneous hollow cylinders under internal and external loading have been solved using the spline-collocation, Fourier-series, and finite-element methods. The results obtained by these methods have been compared. The distribution of displacements depending on the elastic modulus, type of loading, and boundary conditions at the ends of the cylinder has been plotted. The numerical results obtained have been analyzed.

REFERENCES

1. O. C. Zienkiewicz, *The Finite-Element Method in Engineering Science*, McGraw-Hill, New York (1971).
2. V. I. Kozlov and S. N. Yakimenko, "Thermomechanical behavior of viscoelastic solids of revolution during axisymmetric harmonic deformation," *Int. Appl. Mech.*, **25**, No. 5, 443–448 (1989).

3. V. Birman and L. W. Byrd, “Modeling and analysis of functionally graded materials and structures,” *Appl. Mech. Rev.*, **60**, 195–215 (2009).
4. E. Ghafoori and M. Asghari, “Three-dimensional elasticity analysis of functionally graded rotating cylinders with variable thickness profile,” in: *Proc. Institute of Mechanical Engineers*, *Part C: J. Mech. Eng. Sci.*, **226**, No. 3, 585–594 (2012).
5. A. Ya. Grigorenko, A. S. Bergulev, and S. N. Yaremchenko, “Numerical solution of bending problems for rectangular plates,” *Int. Appl. Mech.*, **49**, No. 1, 81–94 (2013).
6. Ya. M. Grigorenko and A. Ya. Grigorenko, “Static and dynamic problems for anisotropic inhomogeneous shells with variable parameters and their numerical solution (review),” *Int. Appl. Mech.*, **49**, No. 2, 123–193 (2013).
7. A. Ya. Grigorenko, W. H. Muller, R. Wille, and S. N. Yaremchenko, “Numerical solution of the problem on the stress-strain state in hollow cylinders using spline-approximations,” *J. Math. Sci.*, **180**, No. 2, 135–145 (2012).
8. A. Ya. Grigorenko, O. V. Vovkodav, and S. N. Yaremchenko, “Stress–strain state of nonthin spherical shells of variable thickness under localized loads,” *Int. Appl. Mech.*, **49**, No. 3, 315–321 (2013).
9. Ya. M. Grigorenko, A. Ya. Grigorenko, and G. G. Vlaikov, *Problems of Mechanics for Anisotropic Inhomogeneous Shells on the Basis of Different Models* [in Russian], Akademperiodika, Kyiv (2009).
10. M. Kashtalyan, “Three-dimensional elasticity solution for bending of functionally graded rectangular plates,” *Europ. J. Mech.- A/ Solids*, **23**, No. 5, 853–864 (2004).
11. M. Koizumi, “The concept of FGM ceramic transactions,” *Funct. Gradient. Mater.*, **34**, 3–10 (1993).
12. Y. Miyamoto, W. A. Kaysser, B. H. Rabin, A. Kawasaki, and R. G. Ford, *Functionally Graded Materials*, *Design*, *Processing and Applications*, Kluwer Academic Publishers, Boston (1999).
13. S. Suresh and A. Mortensen, *Fundamentals of Functionally Graded Materials*, Maney, London (1998).
14. B. Woodward and M. Kashtalyan, “Three-dimensional elasticity solution for bending of transversely isotropic functionally graded plates, *Europ. J. Mech.- A/Solids*, **30**, No. 5, 705–718 (2011).